Characteristics of a GaN-based Gunn diode for THz signal generation*

R K Parida[1], N C Agrawala[2], G N Dash[3], and A K Panda[4,†]

[1]ITER, Siksha 'O' Anusandhan University, Bhubaneswar, Odisha, 751030, India
[2]Rengali College, Sambalpur, Odisha, India
[3]Sambalpur University, Sambalpur, Odisha, 768019, India
[4]National Institute of Science & Technology, Berhampur, Odisha, 761008, India

Abstract: A generalized large-signal computer simulation program for a Gunn oscillator has been developed. The properties of a Gunn diode oscillator based on the widely explored GaN, are investigated using the developed program. The results show some interesting properties in GaN Gunn diodes which are not seen in GaAs and InP diodes. An output power of 1400 kW/cm^2 is achieved from the GaN Gunn diode, as compared to 4.9 kW/cm^2 from a GaAs diode.

Key words: Gunn devices; semiconductor diodes; semiconductor materials; power; GaN
DOI: 10.1088/1674-4926/33/8/084001 **EEACC:** 2570

1. Introduction

Wide bandgap semiconductors like GaN and compounds based on it have recently been established as technologically important materials for both electronic and optoelectronic devices to obtain high power[1−3]. High power GaN-based transistors[4,5] and even high-frequency devices such as GaN-based IMPATTs[6,7], with excellent electrical characteristics, have been reported recently. Major important properties for electronic applications of this material include[8] a large value of wide band gap (3.4 eV), high electrical breakdown field ($E_v \approx 2$ MV/cm), high saturation velocity of electrons ($v_{sn} \approx 2 \times 10^7$ cm/s), and high thermal conductivity (nearly two times that of GaAs). The fundamental properties of GaN indicate that it also exhibits a transferred electron effect[8]. Increased electrical strength, a higher threshold field, and the possibility of faster operation due to a larger electron velocity and reduced energy-relaxation time are expected to be the key features of GaN against traditional III–V semiconductors[8]. The increased value of E_{th} (threshold field) is caused by a large separation between the high and low mobility valleys in GaN ($\Delta E \approx 2.1$ eV) compared to 0.3 eV in GaAs. Studies have shown that the energy relaxation time in GaN is far shorter than that in GaAs. Intuitively, from these fundamental properties of GaN, it is expected that a Gunn diode using this material would manifest a much higher output capability in the mm-wave and tera-hertz range than the traditional GaAs and InP-based Gunn diodes explored so far. To the best of our knowledge, the feasibility of using GaN in a Gunn diode has not yet been explored, with the exception of a few preliminary works[9−11]. Many research groups are of course busy trying to fabricate GaN-based Gunn diodes. A recent report in this regard is not only encouraging but is notable[11]. However, the issues, which play key roles in the realization of a Gunn diode and its high power generation capability, like the presence of a notch near the cathode[12], reverse injection, heterostructure near cathode etc. need to be discussed rigorously before the material can be used in the fabrication of Gunn diodes. Hence a detailed and systematic study has become essential at the present stage to recognize the potentials of GaN and its compounds for use as Gunn diodes at mm-wave and tera-hertz frequency ranges.

Keeping all this in mind, the authors have reported here a detailed theoretical study on GaN-based Gunn devices. The results have been compared with those obtained from GaAs and its compound based Gunn diode operating under similar conditions. Computer software has been developed to study the dynamic properties of such devices. The developed program is a generalized one and can be used at any operating conditions and for any type of Gunn device structure (such as flat profile, notch profile and heterostructure). The results show that GaN Gunn diodes can offer twice/thrice the frequency capability of the GaAs Gunn diodes (90 GHz versus 40 GHz), while their output power density can go as high as 2×10^6 W/cm^2 compared to $\sim 10^3$ W/cm^2 for the GaAs devices. The reported improvements in the mm-wave performance are supported by the high value of the GaN pf^2z figure-of-merit, which is 50–100 times higher than that for GaAs, indicating a strong potential of GaN for microwave signal generation. The developed simulation method and its validity are discussed in the next section.

2. Simulation method

We have developed a versatile and explicit numerical technique based on the first principle approach of the device, which accurately predicts the device characteristics agreeing well with experimental values measured for operating devices. A one-dimensional model is considered to study the domain dynamics in the device because the domain propagation occurs between the parallel contacts, and because the length of the uniformly doped active n-layer is typically much smaller than the

* Project supported by Department of Science and Technology, Government of India through SERC, FIST and TIFAC Program. The fourth author acknowledges the Regular Associate award of ICTP, Trieste, Italy.
† Corresponding author. Email: akpanda62@hotmail.com
Received 21 January 2012, revised manuscript received 6 April 2012

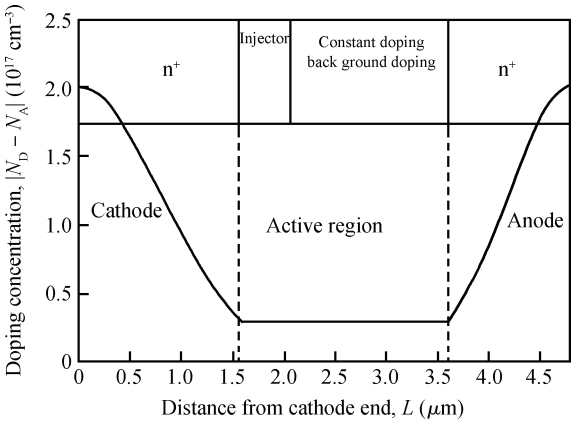

Fig. 1. Typical structure and doping profile of a GaN/AlGaN type Gunn diode.

device diameter. A schematic of structural model with the doping profile used in the computer simulation is shown in Fig. 1.

A finite difference numerical method is developed to solve the carrier continuity equation, Poisson's equation, and space charge equation with a realistic velocity-field characteristic in the device. The field dependent diffusion is taken into consideration. The velocity field characteristics and all other material parameters used here are same as those used in Refs. [6, 7] for GaN-based IMPATTs.

The simulation is initiated by dividing the sample into small cells of finite width in space. The charge and field are regarded as constant within a cell and are evaluated at regular time intervals. The cells in time and space are made small enough to obtain an accurate solution. Taking the initial values of n (electron concentration) and E (electric field) from the cathode contact end, they are updated in each cell. Finally the end value of E is compared with that dictated by the boundary conditions. The boundary conditions can be either in terms of voltage or current. We have used the voltage boundary condition, which requires the integral of the electric field across the device to be equal to the applied DC voltage (V_{dc}). Other conditions, like the device contacts being ohmic and the total current density being continuous throughout the device, are also taken into consideration. The electric field boundary conditions at the outer metal contact edges of the n$^+$ region (anode and cathode ends) are taken to be zero. Thus the time dependence of the electric field at the two edges of the active region is removed. The limits on the space step (Δx) and time step (Δt) are derived from simple physical considerations. In summary, the device simulation consists of the following.

(1) Update the electric field at the future time step by solving Poisson's equation and satisfying the condition $V^{t+\Delta t} = -\int_0^L E\,\mathrm{d}x$, where, $V^{t+\Delta t}$ = terminal voltage at $t + \Delta t$ and L = device length.

(2) Compute the electron mobility from the velocity-field characteristics and the diffusion coefficient from Einstein's relation at every space step.

(3) Solve the current continuity equation for the carrier concentration at the future time step.

(4) If the simulation time is not reached, repeat all above again from step (1).

The presence of Gunn domains led to fluctuations of voltage and current, which gradually built-up into sustained large-signal oscillations. This voltage $V(t)$ and current $I(t)$ waveforms corresponding to sustained oscillations were subjected to harmonic analysis and the resulting power spectrum was used to determine the frequency and power of the Gunn diode oscillators. The details are described below.

The fluctuations in terminal voltage can be represented as:

$$V(t) = V_{dc} + V_{rf}\sin(\omega t). \tag{1}$$

The current density across the device is expressed as

$$J_T(x,t) = qn(x,t)v(x,t) + \varepsilon\frac{\partial E(x,t)}{\partial t}. \tag{2}$$

Integrating Eq. (2) over the length of the device results in

$$\int_0^w J_T(x,t)\mathrm{d}x = \int_0^w qn(x,t)v(x,t)\mathrm{d}x + \frac{\varepsilon}{W}\int_0^w \frac{\partial E(x,t)}{\partial t}\mathrm{d}x. \tag{3}$$

The first term on the right-hand side corresponds to the average particle current density $J_p(t)$ and the second term to the displacement current density. For the purpose of determining the device performance it is only necessary to consider the first term. The second term through device cold capacitance can then be added to the equivalent circuit if necessary. The resulting particle current density can be Fourier analyzed to extract the dc and the fundamental components as follows. The particle current density $J_p(t)$ can be written as $J_p(t) = J_{dc} + J_{rf}(t)$, where

$$J_{dc} = \frac{1}{T}\int_0^T J_p(t)\mathrm{d}t, \tag{4}$$

$$J_{rf}(t) = a_1\cos(\omega t) + b_1\sin(\omega t). \tag{5}$$

The Fourier components a_1 and b_1 can be written as

$$a_1 = \frac{2}{T}\int_0^T J_p(t)\cos(\omega t)\mathrm{d}t, \tag{6}$$

$$b_1 = \frac{2}{T}\int_0^T J_p(t)\sin(\omega t)\mathrm{d}t. \tag{7}$$

The device admittance per unit area is given as

$$Y_D = -G_D + \mathrm{j}B_D, \tag{8}$$

where

$$G_D = \frac{b_1}{V_{rf}}, \tag{9}$$

and

$$B_D = \frac{a_1}{V_{rf}} + \frac{\omega\varepsilon}{W}. \tag{10}$$

The generated RF power is given by

$$P_{rf} = \frac{1}{2}V_{rf}^2 A G_D, \tag{11}$$

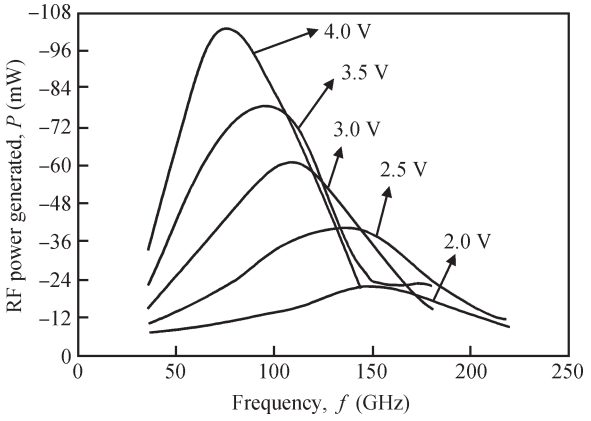

Fig. 2. Frequency versus RF power obtained from different GaAs-based Gunn diodes for verification with experimental results.

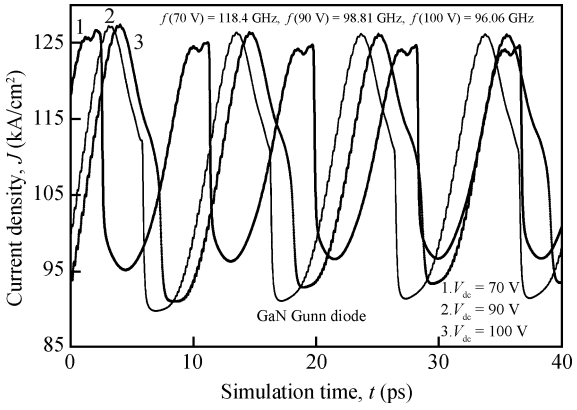

Fig. 3. Simulation time versus current density showing oscillation in a GaN Gunn diode.

where A is the device area. From here the DC to RF conversion efficiency can be calculated as $P_{\rm rf}/P_{\rm dc}$ where $P_{\rm dc} = V_{\rm dc} I_{\rm dc}$ and $I_{\rm dc}$ can be calculated from Eq. (4). Thus the power obtained and DC to RF conversion efficiency for any type of Gunn diode can also be computed by using our simulation program.

The v–E characteristics of GaN used for this study were based on the Monte Carlo simulation results of Albrecht *et al.*[8, 13]. The separation between the high and low mobility valleys (ΔE), the effective mass (m^*) and other material parameters for GaN are taken from different experimental reports. The energy-relaxation time ($\tau_{\rm ER}$) was calculated from $\tau_{\rm ER} = (2m^*\delta E/qE_{\rm th})^{0.5}$ and the inter-valley transfer relaxation time $\tau_{\rm ET}$ was evaluated from the results of Monte Carlo studies by Albrecht *et al.*[8, 13]. Most of the material parameters of GaN are taken from those used in Refs. [6, 7] and references therein. All the material parameters used for GaAs and AlGaAs are taken from experimental reports which are summarized in the MEDICI manual[14].

3. Validity of the model and results

The authenticity of the model developed is also verified. The validity of our computer simulation method is described here by comparing our results with some available experimental results on GaAs-based Gunn diodes. Thus, in order to show the validity of our model, a Gunn device structure presented in Ref. [15] has been used. The device had an n^+nn^+ GaAs structure which operated between 75 and 110 GHz. We have chosen a similar device structure to operate at 94 GHz. The cathode and anode contacts are of 1.6 μm and 2 μm respectively with a doping concentration of 2×10^{17} cm^{-3}. The active region width is chosen to be 2 μm with a background doping concentration of 3×10^{16} cm^{-3}. An exponential variation of doping has been assumed for the n^+–n transitions. This helps the numerical simulation process by providing a continuous and smooth transition between the low-doped n-layer and the heavily doped n^+ contact layers.

The results obtained from our simulation method are shown in Fig. 2. We obtain a power of 102 mW at 94 GHz corresponding to 96 mW in Ref. [15]. The difference between the two results is due to their design (lower length of active region). Our results are thus in reasonable agreement with those from the others work asserting the validity of our model. It is again tested at second harmonic mode with the structure given by Teng *et al.*[16] and found to be in reasonable agreement with our model. Thus we are expecting to get the expected results from our model for GaN-based devices also.

It may be mentioned here that the first observation of oscillations in GaN Gunn diodes were observed only recently by Yilmazoglu *et al.*[11] though many research groups are trying to fabricate Gunn diodes. The drift velocity obtained from such a device was estimated to be 1.9×10^7 cm/s for a doping concentration of 5×10^{18} cm^{-3}. We have also taken such structures and simulated some of them, the results of which are presented in this paper and are in close agreement for the frequency range. Therefore, the authors feel that the simulation results presented in this paper can be used as first-hand data for making such structures experimentally. Keeping this in mind, as mentioned, different structures are taken into account, simulated and presented in this paper.

4. Design criteria

The Gunn device for the present study was designed using some standard criteria. Gunn domain instability in an electronic device with doping n and thickness L is possible if $nL > 4\,\varepsilon E_{\rm th}/q$[17]. As the threshold field of GaN is very high, nL for GaN can be 30 times higher than that for GaAs. Similarly, to avoid static domain formation, n should not exceed the critical doping concentration. $n_{\rm critical} = \varepsilon E_{\rm th}^2/q$ and thus GaN-based devices can be doped significantly to a higher value. Keeping this in mind, the concentration of a flat profile Gunn diode has been varied from 1×10^{16} cm^{-3} to 5×10^{17} cm^{-3} and the results are presented in the next section. Similarly, the device length is varied from 2.5 to 10 μm to operate at around 94 GHz. The frequency of operation is determined from the current density versus time graph, which has been shown at different biases in Fig. 3 for a sample structure.

This figure shows that the frequency of oscillation as well as the oscillation strength changes with a change in applied bias. The required bias can thus be determined from the graph for a given choice of operating frequency. The diameter of the device is chosen as 50 μm in all these cases.

Table 1. Optimized design parameters for a GaN-based Gunn diode operating at 94 GHz.

Structure	Length of the anode, L_a (μm)	Length of the cathode, L_c (μm)	Length of the active region, L_{active} (μm)	Background doping concentration (cm^{-3})	Active region doping (n) (cm^{-3})	Biasing DC value (V)	Doping of anode and cathode region (cm^{-3})
Structure 1	1.2	0.8	5	10^{13}	10^{16}	90	10^{19}
Structure 2	0.3	0.2	3	10^{13}	10^{17}	90	10^{19}

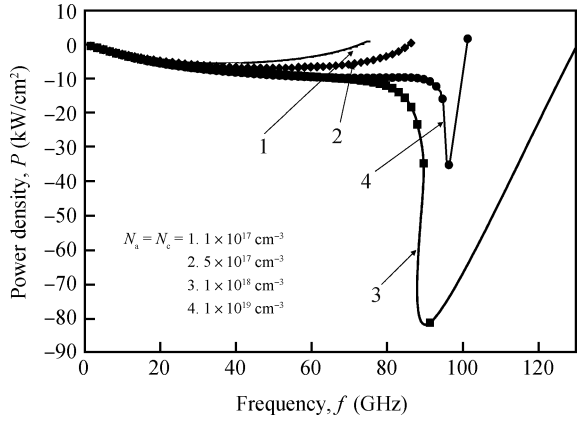

Fig. 4. Frequency versus power density for different values of anode and cathode concentration.

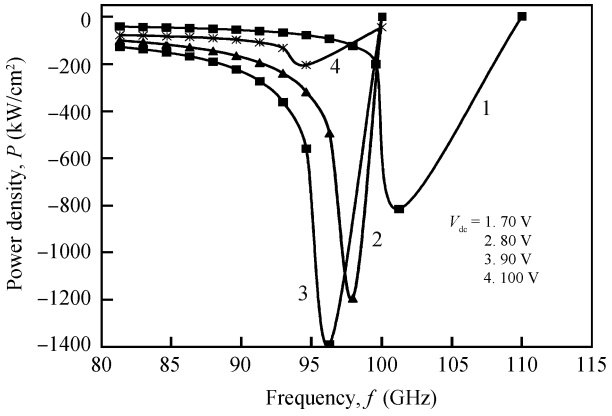

Fig. 6. Frequency versus power density at different applied biases (active length = 3 μm).

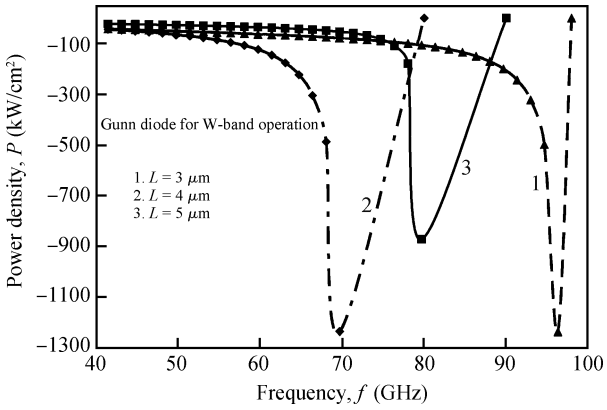

Fig. 5. Frequency versus power density for different active device lengths. The structure is $N_d = 1 \times 10^{17}$ cm^{-3}, $l_a = 0.3$ μm, $l_c = 0.2$ μm.

5. Results and discussion

We have widely varied the structural and operating parameters of the GaN Gunn diode and computed the output power density in each case. The results of our investigation are recorded in Figs. 4, 5, and 6. Figure 4 is a depiction of the effect of cathode/anode doping on the power density of the Gunn diode for a fixed background doping density and bias. In addition, this figure shows the existence of a power output peak at a given frequency and this frequency, for obvious reasons, needs to be chosen as the operating frequency of the Gunn diode oscillator. It is interesting to observe from Fig. 4 that the power density peak gradually steepens with an increase in cathode/anode doping. However, this can not be increased indefinitely and an optimum value needs to be chosen for a good power output.

Figure 5 shows the effect of a change in active region length on the output power density. It is observed that a decrease in the length of an active region records an increase in output power density. However, the length can not be decreased to an arbitrarily lower value because the relation, $nL > 4E_{th}\varepsilon/q$ has to be maintained. Further, for a given choice of frequency of operation the length variation need to be restricted to a limited range. Keeping these points in mind, an optimum value for L has been selected. The applied bias has a definite effect on the output power density. This has been presented in Fig. 6. It is interesting to observe that there is an optimum value of bias for which the power density is maximum; an increase or decrease in bias from this value reduces the power output. The optimized value of bias is chosen from such a graph. Other structural parameters like cathode/anode region length and active region doping density also affect the output power. These parameters have also been varied (graphs not shown for the sake of brevity) and the optimized values in each case have been chosen. All such optimized parameters for two structures are shown in Table 1.

The response time of domain to electric field alternations is important in estimating the maximum signal processing rate of logic devices. The current waveform resulting from bulk nonuniformity is of limited extent and hence the electric field distribution depicting the physical behaviour of the devices at different times of the flow of electrons is shown in Fig. 7. GaN offers higher peak and saturation velocities than GaAs, which leads to an increased transit-time frequency. The threshold and breakdown fields are also large in GaN, which allow operation at a higher bias, leading to an increased output power. The increased electrical strength of GaN also results in a reduced NDR relaxation time, suggesting a higher frequency of opera-

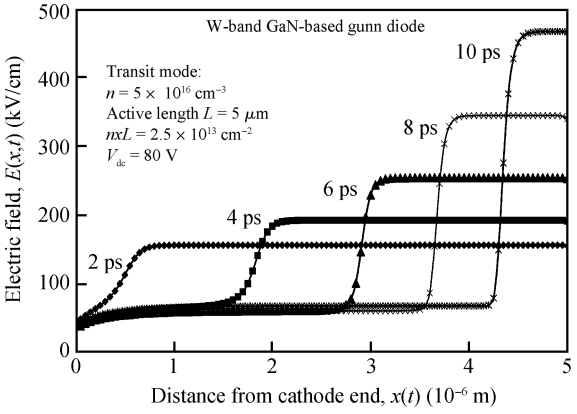

Fig. 7. Gunn electric field formation from the cathode end to the anode end at different time intervals.

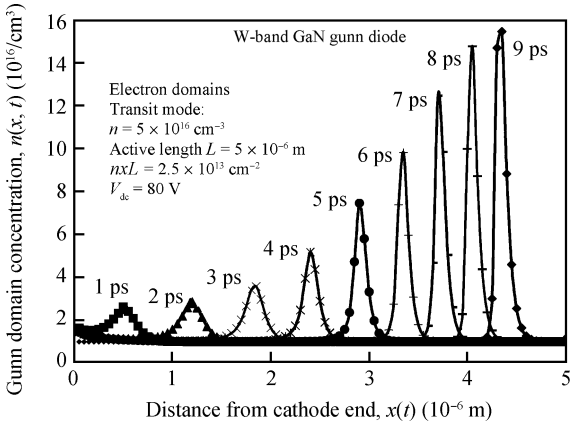

Fig. 8. Gunn domain formation and its movement from the cathode end to the anode end at different time intervals.

tion. When the bias was increased, the oscillation frequency of both the GaN and GaAs oscillators decreased steadily in agreement with the experimental trends observed for GaAs Gunn diodes[18].

The possibility of increased doping in GaN Gunn diodes also leads to a reduction of the differential dielectric relaxation time and as a result, an enhanced growth rate of the Gunn domains. The presence of Gunn domains led to fluctuations of voltage and current, which gradually built-up into sustained large-signal oscillations. This is shown in Fig. 8 for the GaN structure. It is seen that the charge nucleation begins at around 1.0 μm distance from the metal contact (cathode end). Once the charge bunch is formed it slowly travels along the device and begins to grow in size. The charge bunch is then collected at the anode contact. It is seen that the current strength of the GaN-based Gunn diode is a thousand times higher and hence the power delivered/generated is also expected to be higher by the same order of magnitude. To show the strength of the GaN-based Gunn device, the RF power generated by GaAs and GaN-based devices are also compared. The power obtained from GaAs-based Gunn diode (shown in Fig. 2) is 98 mW (4.9 kW/cm^2) where that from GaN based Gunn diode is found to be 27.49 W (1400 kW/cm^2) for a device of 50 μm diameter (on the basis of Fig. 6). This shows a 280 times increase in power generated from a GaN-based Gunn diode compared to

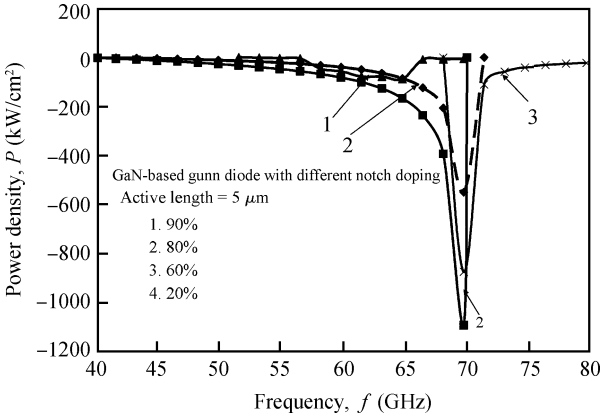

Fig. 9. Power density versus frequency for different notch values in a GaN-based Gunn diode.

the same from the corresponding device based on GaAs.

As noted above and seen from Fig. 8, the Gunn domain starts generating after a distance of around 1.5 μm from the cathode end and hence negative power could not be generated from this region of the cathode end. The presence of this dead zone in the diode impacts negatively on the efficiency of the oscillator, because the length of the active region in which the domain can grow, decreases. Smaller domains translate into smaller output power. Thus optimizing Gun diodes involves decreasing the dead zone. To improve the power performance and to reduce the dead zone, different techniques are used in GaAs-based structures. We have used the same technique here to explore the possibility of generating a higher power output from GaN-based Gunn diodes.

The performance of a standard Gunn diode may be improved by injecting electrons from the cathode end with energy equal to the inter-valley energy difference, E_L, in two ways. Firstly, the dead space–the distance over which the electrons must drift before acquiring sufficient energy to scatter into the L valleys–is reduced to approximately the mean free path for inter-valley scattering. Consequently, electrons may be heated more efficiently, thereby improving device performance. Secondly, the first inter-valley scattering event for electrons entering the drift region is reduced by varying the position at which the characteristic of the Gunn effects are formed[12, 19, 20]. This is usually taken care of by heterostructure, graded barrier, and notch structures[12, 19, 20]. Hence the structures like notch, injection of the charge carrier, and heterostructure are considered here to explore the possibility of improving GaN-based Gunn device performance. The same process has been used for GaAs-based Gunn diodes and the performance has been improved[19, 20]. Therefore, the authors simulate the same kind of device for GaN-based Gunn diodes to obtain generalized information.

The introduction of notch near the cathode to improve the microwave device performance of GaAs and InP-based Gunn diodes has also been used widely. It is one of the methods used to reduce the dead zone, since it forces a high electric field at the notch. This stronger field will accelerate the electrons faster than would otherwise be the case. The electrons will therefore gain enough energy for transfer to the L-valley in a shorter time and distance. The authors have therefore analyzed here the dy-

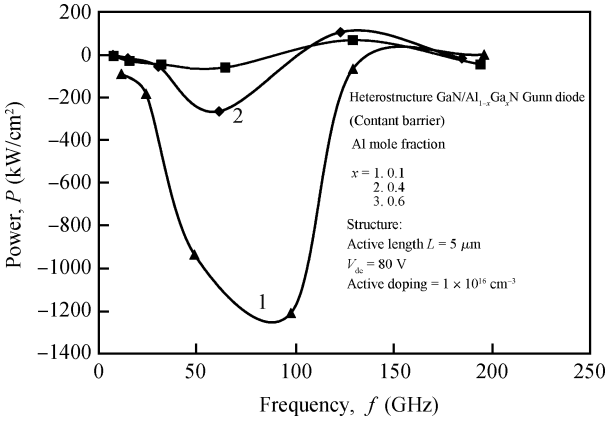

Fig. 10. Heterostructure GaN/AlGaN-based Gunn diode for different values of Al mole fraction.

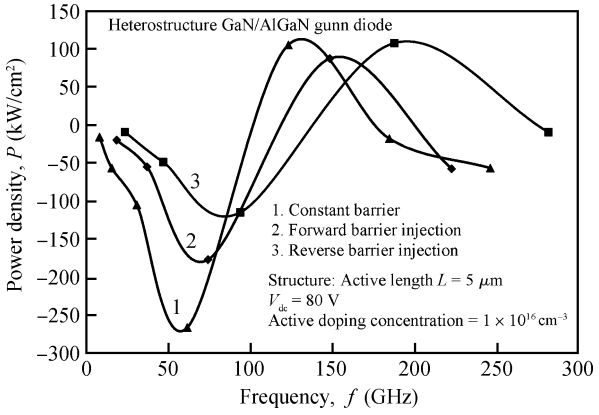

Fig. 11. Heterostructure constant barrier, forward barrier injection and reverse barrier injection in a Gunn diode.

namic properties of GaN-Gunn devices with a notch. When a notch with 20% less doping is considered near the cathode and the same voltage as earlier is applied to the diode, a dipole high-field domain nucleates and travels towards the anode and correspondingly the frequency of the signal generation at the output decreases. However, the power generated improves (as shown in Fig. 9). For comparison, the power output of 900 kW/cm^2 (curve 3 of Fig. 5) in the case of a GaN-based diode without a notch gets enhanced to more than 1100 kW/cm^2 (curve 2 of Fig. 9) when a notch of 20% less doping is introduced to the structure.

However, with further decrease in notch doping, the power output decreases. Similarly an increase of notch doping from 80% also reduces the power output, as may be seen from Fig. 9. Thus an optimum value of notch doping needs to be chosen.

It is also believed that a Gunn diode with hot cathode contacts exhibits improved RF performance. Hence, we have determined here the exact influence of heterojunction cathode contacts on the operating mode. This kind of cathode contact is an injecting one. Over the last few years the injection of hot electrons into GaAs using $Al_xGa_{1-x}As$ has been demonstrated/exploited to enhance the microwave oscillations in a GaAs Gunn diode[19, 20]. Hence, we have also compared here the domain formation characteristics of a heterojunction injection AlGaN/GaN Gunn diode with the conventional Gunn diode. The cathode contact is forward biased when the current flows from the material with the high energy bandgap to the material with the lower energy band gap. The effect of AlGaN/GaN heterostructure on the field stability across a Gunn diode is simulated here for three different kinds of structure, (a) flat/constant AlGaN barrier, (b) forward injection graded AlGaN barrier and (c) reverse injection graded AlGaN barrier[20] and some of the results are presented here (Figs. 10 and 11). First, a constant barrier heterostructure Gunn diode is considered and the Al mole fraction is varied from $x = 0$ to $x = 0.6$ in $Al_{1-x}Ga_xN$. We observe a good power output in the range of $x = 0.1$ and 0.2.

However, the properties degraded with increasing Al mole fraction. Also, the operating frequency decreases with increase in Al mole fraction. At $x = 0.4$, the operating frequency decreases to 65 GHz compared to 99 GHz at $x = 0.1$. This is depicted in Fig. 10.

Next a graded AlGaN injector is considered. For this, the doping profile near the cathode must be carefully controlled so that the field from the ionized impurities in the depletion layer is formed properly when the AlGaN injector is forward biased and does not suppress the formation of the charge instabilities. Keeping it in mind, the Al mole fraction is varied from 0 to 0.5 within a distance from the cathode end to use as injector. The reverse barrier graded junction is also used for the same structure and the results obtained under these three conditions are presented in Fig. 11. It is seen that the oscillation frequency decreases for a constant barrier and forward injection barrier condition. It becomes 65.5 GHz and 74.5 GHz respectively as against 94.5 GHz in reverse barrier case. This trend is consistent with that observed in traditional GaAs and InP-based Gunn diodes[18−20]. The results can be understood in the following way. It can be noted that compared with the conventional structure, the electric field has a stronger variation in the constant and forward barrier case. When injected into the active region, the electrons acquire an energy equivalent to the barrier. Therefore they need to travel a shorter distance to acquire the energy necessary to transfer to the upper valley. This results in a smaller dead zone region.

Further practical GaAs Gunn devices operate at about 3% DC-to-microwave conversion efficiency. This means, the device has to dissipate a large amount of energy in the form of heat. Even with an efficient heat sink, the operating temperatures of practical devices range from about 50 to 200 ℃ for room temperature operation. This heating problem is certainly detrimental to the life and efficiency of these devices. This problem has also been analyzed for a GaN-based Gunn diode to see the potential of a GaN-based Gunn diode at high temperature.

Here we have undertaken a realistic simulation by incorporating material parameters at the actual operating temperatures. For this, the temperature has been varied from 300 to 800 K and the power density has been computed at different temperatures. Curves obtained from such study are shown in Fig. 12. It depicts that the frequency of operation remains the same in all these cases unlike that of GaAs-based Gunn diodes. Though the power generated decreases with an increase in temperature, the dynamic properties remain the same for temperatures up to 400 K. This indicates that GaN-based Gunn diodes

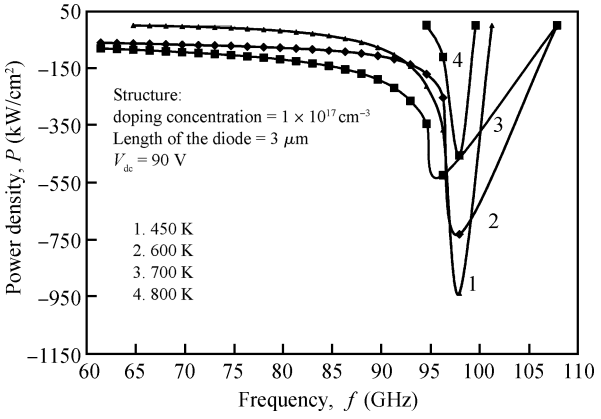

Fig. 12. Effect of temperature on a GaN-based Gunn diode.

can be operated at higher temperature compared to the GaAs based Gunn diodes without a substantial effect on the output power and frequency. Thus, it is expected that the GaN-based Gunn diode can be used as a better oscillator at mm-wave/THz frequency ranges compared to the GaAs-based Gunn diode and our results/structures can be used as first-hand information by experimentalists.

6. Conclusion

A new simulation scheme, starting from the first principle, has been developed. This has been used to simulate some Gunn diodes based on the newly emerging material, GaN. The results obtained have clearly demonstrated the superiority of GaN as a Gunn diode over those based on materials like GaAs and InP. The wider band gap and higher thermal conductivity have boosted the performance of the GaN based Gunn diode. In addition, these properties have also enhanced the thermal tolerance of the device.

References

[1] Litinov V, et al. GaN based Terahertz source. Terahertz and gigahertz electronics and photonics II. Proc SPIE, 2010, 4111: 116
[2] Saad P, Fager C, Cao H, et al. Design of a highly efficient 2–4 GHz Octave band width GaN-HEMT power amplifier. IEEE Trans MTT, 2010, 58 (7): 1677
[3] Esposto M, Chini A, Rajan S. Analytical model for power switching GaN-based HEMT design. IEEE Trans Electron Devices, 2011, 58 (5): 1456
[4] Heller E R, Ventury R, Green D S. Development of a versatile physics-based finite-element model of an AlGaN/GaN HEMT capable of accommodating process and epitaxy variations and a librated using multiple DC parameter. IEEE Trans Electron Devices, 2011, 58(4): 1091
[5] Lenka T R, Panda A K. Role of nanoscale AlN and InN for the microwave characteristics of AlGaN/(Al, In)N/GaN-based HEMT. Semiconductors, 2011, 45(5): 650
[6] Panda A K, Pavlidis D, Alekseev E. DC and high-frequency characteristics of GaN-based IMPATTs. IEEE Trans Electron Devices, 2001, 48: 820
[7] Panda A K, Pavlidis D, Alekseev E. Noise characteristics of GaN-based IMPATTs. IEEE Trans Electron Devices, 2001, 48: 1473
[8] Albrecht J D, Wang R P, Ruden P P, et al. Electronic transport characteristics of GaN for high temperature device modeling. J Appl Phys, 1998, 83(9): 4777
[9] Yang L A, Hao Y, Yao Q, et al. Improved negative differential mobility model of GaN and AlGaN for a Terahertz Gunn diode. IEEE Trans Electron Devices, 2011, 58(4): 1076
[10] Lau K S, Tozer R C, David J P R, et al. Double transit region Gunn diodes. Semicond Sci Technol, 2007, 22: 245
[11] Yilmazoglu O, Mutamba K, Pavlidis D, et al. First observation of bias oscillation in GaN Gunn diodes on GaN substrate. IEEE Trans Electron Devices, 2008, 55: 1563
[12] Yang L, Hao Y, Zhang J. Use of AlGaN in the notch region of GaN Gunn diodes. Appl Phys Lett, 2009, 95: 143507
[13] Albrecht J D, Wang R P, Ruden P P, et al. Electronic transport characteristics of GaN for high temperature device modeling. J Appl Phys, 1999, 83(9): 4777
[14] MEDICI: two dimensional device simulation program, TMA, 1997
[15] Kamaria R. Potential of GaAs and InP Gunn devices at high frequencies. PhD Thesis, University of Michigan, 1992
[16] Teng S J J, Goldwasser R E. High performance second-harmonic operation W-band GaAs Gunn diode. IEEE Electron Device Lett, 1989, 10: 412
[17] Kamoua R, Eisele H, Haddad G I. D-band (110–170 GHz) InP Gunn devices. Solid-State Electron, 1993, 36: 1547
[18] Kal'fa A A, Poresh S B, Tager A S. High frequency limit of the Gunn effect in GaAs. Sov Phys Semicond, 1981, 15: 1343
[19] Greenworld Z, et al. The effect of a high energy injection on the performance of mm-wave Gunn oscillators. Solid-State Electron, 1988, 31: 1211
[20] Couch N R, Spooner H, Beton P H, et al. High performance graded AlGaAs injector GaAs Gunn diodes at 94 GHz. IEEE Electron Device Lett, 1989, 10: 288